Discovery of imidazo[1,5-*a*]pyridines and -pyrimidines as potent and selective RORc inverse agonists

Benjamin P. Fauber, Alberto Gobbi, Kirk Robarge, Aihe Zhou, Adrian Barnard, Jianhua Cao, Yuzhong Deng, Céline Eidenschenk, Christine Everett, Arunima Ganguli, Julie Hawkins, Adam R. Johnson, Hank La, Maxine Norman, Gary Salmon, Susan Summerhill, Wenjun Ouyang, Wei Tang, Harvey Wong

PII: S0960-894X(15)00529-6
DOI: http://dx.doi.org/10.1016/j.bmcl.2015.05.055
Reference: BMCL 22745

To appear in: *Bioorganic & Medicinal Chemistry Letters*

Received Date: 16 April 2015
Revised Date: 18 May 2015
Accepted Date: 21 May 2015

Please cite this article as: Fauber, B.P., Gobbi, A., Robarge, K., Zhou, A., Barnard, A., Cao, J., Deng, Y., Eidenschenk, C., Everett, C., Ganguli, A., Hawkins, J., Johnson, A.R., La, H., Norman, M., Salmon, G., Summerhill, S., Ouyang, W., Tang, W., Wong, H., Discovery of imidazo[1,5-*a*]pyridines and -pyrimidines as potent and selective RORc inverse agonists, *Bioorganic & Medicinal Chemistry Letters* (2015), doi: http://dx.doi.org/10.1016/j.bmcl.2015.05.055

Discovery of imidazo[1,5-*a*]pyridines and -pyrimidines as potent and selective RORc inverse agonists

Benjamin P. Fauber,[a,*] Alberto Gobbi,[a] Kirk Robarge,[a] Aihe Zhou,[a] Adrian Barnard,[b] Jianhua Cao,[c] Yuzhong Deng,[a] Céline Eidenschenk,[a] Christine Everett,[a] Arunima Ganguli,[b] Julie Hawkins,[b] Adam R. Johnson,[a] Hank La,[a] Maxine Norman,[b] Gary Salmon,[b] Susan Summerhill,[b] Wenjun Ouyang,[a] Wei Tang,[c] and Harvey Wong[a]

[a] Genentech, Inc., 1 DNA Way, South San Francisco, California 94080, USA

[b] Argenta, Units 7-9 Spire Green Centre, Flex Meadow, Harlow, Essex, CM19 5TR, UK

[c] ChemPartner, No. 5 Building, 998 Halei Road, Zhangjiang Hi-Tech Park Pudong New Area, Shanghai China, 201203

Corresponding Author:

Benjamin P. Fauber

Genentech, Inc.

1 DNA Way, South San Francisco, CA 94080, USA

E-mail address: Fauber.Benjamin@gene.com

Telephone: +1-650-467-5773

Abstract.

The nuclear receptor (NR) retinoic acid receptor-related orphan receptor gamma (RORγ, RORc, or NR1F3) is a promising target for the treatment of autoimmune diseases. RORc is a critical regulator in the production of the pro-inflammatory cytokine interleukin-17. We discovered a series of potent and selective imidazo[1,5-*a*]pyridine and -pyrimidine RORc inverse agonists. The most potent compounds displayed >300-fold selectivity for RORc over the other ROR family members, PPARγ, and NRs in our cellular selectivity panel. The favorable potency, selectivity, and physiochemical properties of GNE-0946 (**9**) and GNE-6468 (**28**), in addition to their potent suppression of IL-17 production in human primary cells, support their use as chemical biology tools to further explore the role of RORc in human biology.

Keywords: RORc; RORγ; IL-17; PPARγ; GNE-0946; GNE-6468.

Inhibiting the function of interleukin (IL)-17 with anti-IL-17 antibodies has proven successful in the treatment of psoriasis,[1-3] rheumatoid arthritis (RA),[4] ankylosing spondylitis,[5] and uveitis.[6] IL-17 is a validated target for the treatment of psoriasis. IL-23 lies upstream of IL-17 and anti-IL-12/23 antibodies (*e.g.* ustekinumab)[7] have demonstrated efficacy in the treatment of moderate-to-severe psoriasis. The recent FDA approval of the anti-IL-17 antibody secukinumab[8] for the treatment of moderate-to-severe plaque psoriasis further highlighted the importance of the IL-17 pathway in autoimmune diseases.[9-10] The nuclear receptor (NR) retinoic acid receptor-related orphan receptor gamma (RORγ or RORc, also known as NR1F3)[11] is an important regulator in the production of IL-17.[12] RORc also plays a role in production of IL-22[13] and cytokines from innate lymphoid cells (ILCs)[14-15] and γδ T cells.[16] Based on the influence of RORc over multiple inflammatory pathways, it has been proposed that RORc is a valuable molecular target for the treatment of inflammatory diseases.[17-23]

Our group has previously reported the discovery and optimization of tertiary sulfonamide RORc inverse agonists.[24-27] In 2012, Organon (Merck) disclosed an acyl-indazole series of RORc inverse agonists.[28] This disclosure led us to investigate an exemplary acyl-indazole compound from Organon (**1**, Table 1) in a time-resolved fluorescence biochemical assay that monitored the ability of the human RORc ligand binding domain (LBD) to bind to a co-activator peptide derived from steroid receptor co-activator-1 (SRC1).[29] Compounds that disrupted the recruitment of the SRC1 co-activator peptide were RORc inverse agonists. Compound **1** was a potent inverse agonist in the RORc SRC1 biochemical assay (EC_{50} = 16 nM).

Compounds with structures similar to **1** have been reported as potent peroxisome proliferator-activated receptor (PPAR)-γ ligands,[30] which led us to profile **1** in a biochemical assay that monitored the ability of a compound to displace a fluorescent probe from the human

PPARγ-LBD.[31] In this PPARγ competitive binding assay, **1** displayed a strong affinity for human PPARγ (IC_{50} = 130 nM). The PPARγ potency of **1** was superior to the FDA-approved PPARγ agonists pioglitazone[32] (IC_{50} = 720 nM) and troglitazone[33] (IC_{50} = 340 nM), as measured in our PPARγ binding assay. Due to the potential risks associated with the modulation of PPARγ,[34] we designed new analogs with the goal of improving selectivity for RORc over PPARγ (as compared with **1**) through the exploration of alternative cores to the 1-acyl-indazole motif embedded in **1**.

In our exploration of different core motifs, we attempted to preserve the 1- and 3-position vectors of the azole core for the 4'-benzoic acid and keto-arene groups, respectively. We also prioritized cores that removed the potential metabolic liability of the 1-acyl-indazole moiety, as related compounds have demonstrated *in vivo* instability.[35] The imidazo[1,5-*a*]pyridine analog[36] (**2**, Table 1) fulfilled these criteria and also provided an analog with improved RORc inverse agonist potency (EC_{50} = 10 nM) in comparison to **1**. Compound **2** also possessed a superior ligand-lipophilicity efficiency (LLE)[37-38] in comparison to **1** (**2** LLE = 6.5, **1** LLE = 4.9) and an improved selectivity for RORc over PPARγ (PPARγ IC_{50} = 1.5 μM). Saturation of the pyridine ring in **2** provided a 5,6,7,8-tetrahydro-imidazo[1,5-*a*]pyridine analog (**3**) and resulted in a reasonable RORc inverse agonist potency (EC_{50} = 58 nM) with an LLE value (LLE = 6.4) and PPARγ affinity (PPARγ IC_{50} = 2.1 μM) comparable to **2**. Synthesis of an imidazo[1,5-*a*]pyrimidine analog (**4**) provided a modest RORc inverse agonist (EC_{50} = 84 nM) and further decreased the affinity for PPARγ (IC_{50} = 4.2 μM). The imidazo[1,5-*a*]pyrazine analog (**5**) possessed a substantially diminished RORc inverse agonist activity (EC_{50} = 2.6 μM) in comparison to **4**. Further core changes such as the 3-acyl-tetrahydroindazole (**6**), imidazo[1,2-*a*]pyrazine (**7**), and 5,6,7,8-tetrahydro-imidazo[1,2-*a*]pyran (**8**) were devoid of

detectable RORc inverse agonist activity at concentrations up to 10 μM. The difference in RORc potency between **3** and **6** was striking given their structural similarities. We rationalized this difference in that the nitrogen atoms in the core of **3** do not form a resonance contribution to the ketone group, whereas, **6** does allow a resonance contribution into the ketone from the core N1 nitrogen atom. These differences in resonance contributions between the cores of **3** and **6** could have an impact on the Lewis basicity of the respective ketone functional groups and thus, how they complement the RORc-LBD ligand binding pocket.

Table 1

SAR of core changes

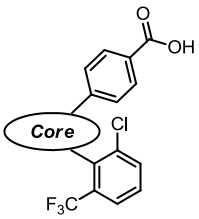

Compd	Core	RORc SRC1 EC_{50}[a] (μM) [%eff]	LLE[b]	LogD (pH 7.4)	PPARγ IC_{50}[c] (μM)
1	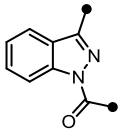	0.016 [-99%]	4.9	2.9	0.13
2	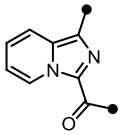	0.010 [-99%]	6.5	1.5	1.5
3	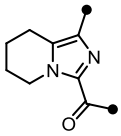	0.058 [-99%]	6.4	0.8	2.1
4	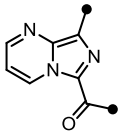	0.084 [-99%]	6.8	0.3	4.2
5	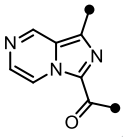	2.6 [-75%]	4.9	0.7	ND
6	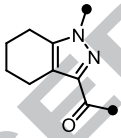	>10	-	-0.3	ND
7	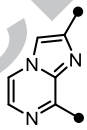	>10	-	1.0	ND
8	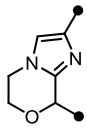	>10	-	1.0	ND

See the Supplementary Data for experimental details associated with each assessment. All assay results are reported as the geometric mean of at least two separate runs. ND = not determined. [a]Inhibition of RORc-LBD recruitment of the SRC1 co-activator peptide; negative percent efficacy denotes inverse agonism relative to the basal activity of

apo-RORc-LBD. [b]Ligand-lipophilicity efficiency (LLE) was calculated using the equation: (RORc SRC1 pEC_{50}) – LogD (pH 7.4).[37-38] [c]Binding assay monitored the displacement of a fluorescent probe from the PPARγ-LBD.

The favorable profile of **2** led us to focus on the imidazo[1,5-*a*]pyridine core. We explored the replacement of the carboxylic acid group in **2** with a range of amides, heterocyclic carboxylic acid isosteres, and *N*-acylsulfonamides. These analogs were devoid of detectable RORc inverse agonist activity at concentrations up to 10 μM. Due to the importance of the 4'-carboxylic acid group in maintaining RORc inverse activity, we sought to explore the substitution and modification of the 4'-benzoic acid moiety (Table 2). Introduction of a phenol at the 3'-position of the ring (**9**, GNE-0946) resulted in an approximate fivefold improvement in RORc inverse agonist potency (EC_{50} = 2 nM) over **2**, but **9** also had an increased PPARγ affinity (IC_{50} = 650 nM). Introduction of fluorine at 2'-position on the arene (**10**) provided an analog with similar RORc inverse agonist activity as **2** and an increased affinity for PPARγ (IC_{50} = 320 nM). Similar improvements in RORc potency were also noted in the Organon (Merck) patent application[28] with the installation of these 3'-phenol and 2'-fluorine groups, respectively, into analogs of **1**.

Fluorine was the preferred 2'-position substituent as chlorine, cyano, and methyl groups were >100-fold less potent in the RORc SRC1 biochemical assay. Synthesis of the cyclohexene carboxylic acid analog (**11**) resulted in an approximate tenfold loss of RORc inverse agonist activity as compared with **2**. The cyclohexane carboxylic acid analogs (**12** and **13**) resulted in a further loss of RORc inverse agonist potency, with the 1',4'-*trans* diastereomer (**12**) as the preferred stereoisomer (EC_{50} = 400 nM). Introduction of a piperidine 4'-carboxylic acid (**14**) provided a compound of similar RORc inverse agonist potency to **12**, with no detectable affinity for PPARγ up to concentrations of 10 μM. Various hydroxy-piperidine analogs were explored in

an attempt to restore some RORc potency, as similar changes (*i.e.*, **2** to **9**) have previously led to a fivefold improvement in potency. Introduction of an alcohol at the 4'-position (**15**) led to a tenfold loss of potency (EC_{50} = 6.8 μM) as compared with **14**. Placement of the alcohol group at the 3'-position led to improvements in potency, with the *trans* diastereomers being tenfold more potent than the *cis* diastereomers. Separation of the *trans* diastereomers into the two separate enantiomers with unknown absolute stereochemistry led to compounds **16** and **17**. Compound **17** possessed an approximate fivefold improvement in RORc inverse agonist potency (EC_{50} = 97 nM) as compared with **14**.[40] Compound **17** also had no detectable affinity for PPARγ up to concentrations of 10 μM. Although the RORc potency, LLE, and selectivity profile of **17** was encouraging, the approximate tenfold difference in RORc potency as compared with **2** led us to focus on the 4'-benzoic acid motif in subsequent analogs.

Table 2

SAR of the imidazo[1,5-*a*]pyridine 1-position

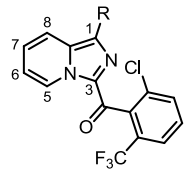

Compd	R	RORc SRC1 EC_{50}[a] (μM) [%eff]	LLE[b]	LogD (pH 7.4)	PPARγ IC_{50}[c] (μM)
9	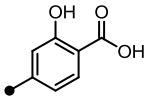	0.002 [-99%]	6.2	2.5	0.65
10	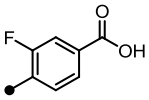	0.009 [-99%]	6.2	1.8	0.32
11	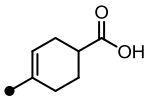	0.10 [-99%]	5.5	1.5	1.8
12	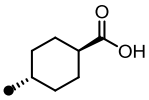	0.40 [-90%]	5.1	1.3	ND
13	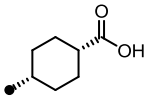	4.3 [-73%]	3.5	1.8	ND
14	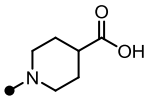	0.54 [-94%]	5.9	0.4	>10
15	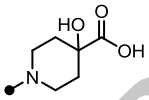	6.8 [-56%]	5.1	0	ND
16[d]	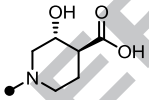	0.44 [-95%]	6.1	0.3	>10
17[d]	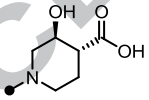	0.097 [-98%]	6.6	0.4	>10

See the Supplementary Data for experimental details associated with each assessment. All assay results are reported as the geometric mean of at least two separate runs. ND = not determined. [a]Inhibition of RORc-LBD recruitment of the SRC1 co-activator peptide; negative percent efficacy denotes inverse agonism relative to the basal activity of apo-RORc-LBD. [b]Ligand-lipophilicity efficiency (LLE) was calculated using the equation: (RORc SRC1 pEC_{50}) – LogD (pH 7.4).[37-38] [c]Binding assay monitored the displacement of a fluorescent probe from the PPARγ-LBD. [d]Single enantiomers of the *trans* diastereomers with unknown absolute stereochemistry; the stereochemistry at the 3'- and 4'-positions of the piperidine ring was arbitrarily assigned.

In parallel to our exploration of the SAR on the 1-(4'-benzoic acid) group, we also evaluated a series of changes to the 3-acylarene moiety (Table 3). For this endeavor, we chose the 5,6,7,8-tetrahydro-imidazo[1,5-*a*]pyridine core (similar to **3**) as our prior studies[26] had shown that minimizing the aromatic ring count of RORc ligands can lead to improvements in selectivity and ADME properties. Removal of the 2'-chlorine on the 3-acylarene of **18** led to an approximate 25-fold loss of potency (**19**, EC_{50} = 0.84 μM). We explored other analogs that replaced the 2',6'-disubstitution with substituents elsewhere on the 3-acylring and these compounds had no detectable potency (up to a 10 μM concentration) in the RORc biochemical assay. Thus, we focused our efforts on 2',6'-disubstituted arenes with the goal of minimizing the overall lipophilicity of the analogs. Replacement of the 6'-(trifluoromethyl) group on the arene with a range of substituents including fluorine (**20**), chlorine (**21**), cyano (**22**), and methoxy (**23**) all led to a loss of RORc potency with no improvements in LLE relative to **18**. The calculated LogP (cLogP)[39] value of the 2-chloro-6-cyclopropylarene analog (**24**) suggested that this compound was less lipophilic than **18** (**24** cLogP = 6.2, **18** cLogP = 6.4). The measured LogD (pH 7.4) values indicated that **24** was slightly more lipophilic than **18** (**24** LogD = 1.6, **18** LogD = 1.3) and **24** was a more potent RORc inverse agonist (EC_{50} = 27 nM). Additionally, **24** possessed an improved PPARγ selectivity profile in comparison to **18**. Replacement of the 2'-chloro group on the 3-acylarene with cyano (**25**) or methoxy (**26**) substituents provided analogs that were significantly less potent in the RORc SRC1 biochemical assay. We also explored a range of *ortho*- and *ortho*/*ortho*-disubstituted heteroaromatic rings and only the 3',5'-dichloro-pyridine analog (**27**) demonstrated a detectable level of RORc inverse agonist

activity (EC_{50} = 0.51 μM). In sum, there appeared to be a strict requirement for lipophilic 2',6'-disubstitution on the 3-acylarene group.

Table 3

SAR of the 3-acylarene group

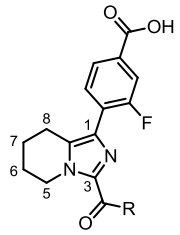

Compd	R	RORc SRC1 EC_{50}[a] (μM) [%eff]	LLE[b]	LogD (pH 7.4)	PPARγ IC_{50}[c] (μM)
18	2'-Cl-6'-CF_3-Ph	0.032 [-96%]	6.2	1.3	0.76
19	2'-CF_3-Ph	0.84 [-96%]	4.7	1.4	5.6
20	2'-Cl-6'-F-Ph	0.19 [-99%]	5.5	1.2	2.9
21	2',6'-diCl-Ph	0.077 [-99%]	5.7	1.5	1.1
22	2'-Cl-6'-CN-Ph	0.25 [-99%]	5.9	0.7	7.7
23	2'-Cl-6'-MeO-Ph	0.24 [-98%]	5.8	0.8	5.5
24	2'-Cl-6'-(*c*-Pr)-Ph	0.027 [-99%]	5.9	1.6	1.3
25	2'-CN-6'-CF_3-Ph	0.22 [-99%]	5.9	0.7	>10
26	2'-OMe-6'-CF_3-Ph	0.67 [-96%]	-	ND	9.1
27	3',5'-diCl-pyridyl	0.51 [-98%]	5.2	1.1	4.2

See the Supplementary Data for experimental details associated with each assessment. All assay results are reported as the geometric mean of at least two separate runs. ND = not determined. [a]Inhibition of RORc-LBD recruitment of the SRC1 co-activator peptide; negative percent efficacy denotes inverse agonism relative to the basal activity of apo-RORc-LBD. [b]Ligand-lipophilicity efficiency (LLE) was calculated using the equation: (RORc SRC1 pEC_{50}) – LogD (pH 7.4).[37-38] [c]Binding assay monitored the displacement of a fluorescent probe from the PPARγ-LBD.

After exploring the core, 1-position substituents, and the optimal substitution of the 3-acylarene group, we prioritized the optimal substituents that possessed favorable potency and selectivity for RORc over PPARγ. Combining these optimal substituents into one compound (**28**, GNE-6468, Table 4) provided a highly potent RORc inverse agonist (EC_{50} = 2 nM) with >1,000-fold selectivity for RORc over PPARγ. Compound **28** also had the highest LLE value

(LLE = 7.2) of all the compounds we profiled. We then tested the potent RORc inverse agonists with favorable RORc selectivity over PPARγ in a series of ROR and NR cell-based assays to further explore their cellular potencies and selectivity profiles.

Table 4

Combination of favored substituents into one analog

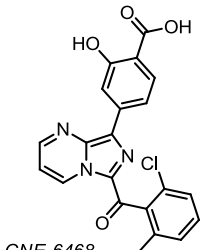

GNE-6468
(**28**)

RORc SRC1 EC_{50}[a] (μM) [%eff]	LLE[b]	LogD (pH 7.4)	PPARγ IC_{50}[c] (μM)
0.002 [-99%]	7.2	1.5	3.4

See the Supplementary Data for experimental details associated with each assessment. All assay results are reported as the geometric mean of at least two separate runs. [a]Inhibition of RORc-LBD recruitment of the SRC1 co-activator peptide; negative percent efficacy denotes inverse agonism relative to the basal activity of apo-RORc-LBD. [b]Ligand-lipophilicity efficiency (LLE) was calculated using the equation: (RORc SRC1 pEC_{50}) – LogD (pH 7.4).[37-38] [c]Binding assay monitored the displacement of a fluorescent probe from the PPARγ-LBD.

We examined **2**, **9**, **10**, **18**, **24**, and **28** in a series of HEK-293 cell Gal4-ROR construct human NR-dependent transcriptional reporter assays (Table 5). We profiled the three isoforms of human ROR (RORc, RORb, and RORa) by monitoring the suppression of their basal transcriptional activity in the absence of any exogenous agonist.[29] In order to assess the NR cellular selectivity of the potent RORc inverse agonists, we also tested these compounds in a panel of cellular reporter assays of human farnesoid X receptor (FXR), liver X receptor (LXR)-α, LXRβ, and PXR in both agonist mode (no agonist ligand added) and antagonist mode (using

T0901317 [*N*-(2,2,2-trifluoroethyl)-*N*-[4-[2,2,2-trifluoro-1-hydroxy-1-(trifluoromethyl)ethyl]phenyl]-benzenesulfonamide] as an exogenous ligand).[29] All of these compounds demonstrated favorable RORc inverse agonist cellular potency values (EC_{50} = 4-36 nM), with no detectable activity against the other ROR family members (up to 10 μM concentration). In addition, none of these compounds demonstrated detectable activity against the other NRs in our cell assay panel in agonist or antagonist mode (up to 10 μM concentration). These results demonstrated the excellent cellular selectivity profiles of **2**, **9**, **10**, **18**, **24**, and **28** for RORc over other NRs (>277- to >1,000-fold selectivity).

Table 5

RORc potency and selectivity profiles in Gal4 human transcription assays[a]

Compd	RORc Cell EC_{50} (μM)	RORb Cell EC_{50} (μM)	RORa Cell EC_{50} (μM)	FXR Cell EC_{50} (μM)	LXRα Cell EC_{50} (μM)	LXRβ Cell EC_{50} (μM)	PXR Cell EC_{50} (μM)
2	0.013	>10	>10	>10	>10	>10	>10
9	0.004	>10	>10	>10	>10	>10	>10
10	0.010	>10	>10	>10	>10	>10	>10
18	0.036	>10	>10	>10	>10	>10	>10
24	0.026	>10	>10	>10	>10	>10	>10
28	0.013	>10	>10	>10	>10	>10	>10

See the Supplementary Data for experimental details associated with each assessment. All assay results are reported as the geometric mean of at least two separate runs. [a]All assays were conducted in HEK293-Gal4 cellular constructs. All NR assays monitored the suppression of their respective basal transcriptional activities, an outcome consistent with inverse agonist activity of ligands with these receptors.

Based on their favorable RORc cell potency values, we progressed **2**, **9**, **10**, **18**, **24**, and **28** into human PBMC cytokine production assays[29] to assess their abilities to inhibit the production of IL-17 (Table 6). Compounds **2**, **10**, **18**, and **24** displayed modest inhibition of IL-17 production in the human PBMC assay (EC_{50} = 230, 120, 230, and 300 nM, respectively),

whereas **9** and **28** displayed more potent inhibition of IL-17 production (EC_{50} = 17 and 30 nM, respectively). Compounds **9** and **28** possessed a unique substructure in contrast to **2**, **10**, **18**, and **24**, indicating that the 1-(3'-hydroxy-4'-benzoic acid) motif present in **9** and **28** may engender enhanced potency in the IL-17 production assay. It was also noteworthy that none of the compounds showed any activity in interferon (IFN)-γ or CellTiter-Glo® (CTG) counter screen assays, demonstrating that the compounds were not indiscriminately suppressing cytokine production, nor were they grossly cytotoxic.

Compounds **9** and **28** were potent inhibitors of IL-17 production in human PBMC cells (EC_{50} values $\leq$ 30 nM, Table 6), yet they were no more effective in further suppressing the maximum percent inhibition of IL-17 production (%max) than compounds that were an order of magnitude less potent (*i.e.* **2**, **10**, **18**, and **24**). Indeed, we have noted in our previously-disclosed human PBMC data with several RORc inverse agonist chemotypes that the IL-17 PBMC %max values average 77% inhibition (±23% of the %max inhibition value for the 13 different human IL-17 PBMC assay results we have disclosed where the IL-17 PBMC EC_{50} = 0.044-3.0 μM)[24-26,29] The lack of complete suppression of IL-17 production in human PBMCs (*i.e.* IL-17 PBMC %max $\geq$ 99%) may be due to the role of RORa in the production of IL-17. Previous mouse genetic knock-out studies have demonstrated that the production of murine IL-17 is dependent on both murine RORα and RORγ.[41-42] Potent and selective human RORa inverse agonists would be required to explore this hypothesis in the context of human IL-17 production. The deficiency of potent and selective human RORa tool compounds is the focus of several research programs.[21-22]

Table 6

Potency in human IL-17 and IFNγ production assays[a]

Compd	IL-17 PBMC EC_{50} (μM)	IL-17 PBMC %max. inhibition	IFNγ EC_{50} (μM)	CTG EC_{50} (μM)
2	0.23	69%	>10	>10
9	0.017	70%	>10	>10
10	0.12	63%	>10	>10
18	0.23	64%	>10	>10
24	0.30	72%	>10	>10
28	0.030	73%	>10	>10

See the Supplementary Data for experimental details associated with each assessment. All assay results are reported as the mean of at least three separate runs. [a]All assays were conducted using peripheral blood mononuclear cells (PBMCs) isolated from human whole blood. Interferon gamma (IFNγ) and CellTiter-Glo® (CTG) cell culture assays were used as positive controls to monitor for non-T_H17 cell cytokine activity and adverse off-target effects on cell physiology, respectively.

We also evaluated **9** and **28** in a suite of *in vitro* ADME assays (Table 7).[43-44] Compound **9** displayed moderate predicted hepatic clearance (CL_{hep}) values in human and rodent hepatocyte metabolic stability assays (CL_{hep} = 9 and 32 mL/min/kg, respectively), whereas **28** displayed high predicted clearance values in human and rodent hepatocytes (CL_{hep} = 17 and 42 mL/min/kg, respectively). Further profiling of the compounds in human and rat plasma-protein binding (PPB) assays demonstrated that **9** and **28** were highly protein bound in both species (%bound = >99% and 99%, respectively). Compounds **9** and **28** displayed favorable apparent permeability ($P_{app(A\rightarrow B)}$ = 12 and 8×10^{-6} cm/s, respectively) with minimal efflux ($P_{app(A\rightarrow B)}/P_{app(B\rightarrow A)} < 2$) in a Madin-Darby canine kidney (MDCK) cellular permeability assay.[45] Both **9** and **28** were highly soluble as assessed by a kinetic aqueous solubility assay (45-86 μM). Thus, **9** and **28** were highly potent and selective RORc inverse agonists with favorable properties and moderate-to-high clearance values.

Table 7

In vitro ADME profiles

Compd	Hu Hep[a] CL_{hep} (mL/min/kg)	Rat Hep[b] CL_{hep} (mL/min/kg)	Human PPB (%bound)	Rat PPB (%bound)	MDCK P_{app}[c] A→B (10^{-6} cm/s)	MDCK P_{app}[c] B→A (10^{-6} cm/s)	Solubility[d] (μM)
9	9	32	>99	>99	12	10	86
28	17	42	99	99	8	15	45

See the Supplementary Data for experimental details associated with each assessment. [a]Predicted human hepatic clearance values extrapolated from *in vitro* human hepatocyte (Hu Hep) metabolic stability experiment. [b]Predicted rat hepatic clearance values extrapolated from *in vitro* rat hepatocyte (Rat Hep) metabolic stability experiment. [c]Madin-Darby canine kidney (MDCK) cell permeability assay to assess membrane permeability (P_{app}); A→B: apical-to-basolateral, B→A: basolateral-to-apical.[45] [d]Aqueous kinetic solubility at pH 7.4 (measured in a high-throughput assay).

Compound **9** was profiled in a rodent *in vivo* pharmacokinetic (PK) experiment (Table 8) to determine if the *in vitro* rat hepatic clearance estimate (Table 7) was predictive of its *in vivo* clearance value. In a rat PK experiment, **9** demonstrated a high plasma clearance value (CL_p = 130 mL/min/kg) that did not correlate with its *in vitro* clearance value (Rat Hep CL_{hep} = 32 mL/min/kg). The *in vivo* plasma clearance of **9** was in excess of rodent liver blood flow (55 mL/min/kg), indicating that extrahepatic clearance mechanisms[46] may also be participating in the metabolism of **9**.

A very recent set of patent applications from Glenmark Pharmaceuticals[47] describe two series of compounds related to **1**. It is unknown if the compounds in the Glenmark patent applications possess similar metabolic stabilities as those observed with **9** and **28**.

Table 8

Single dose rat *in vivo* PK profile of **9**

Compd	CL_p[a] (mL/min/kg)	V_d[b] (L/kg)	C_{max}[c] (μM)	AUC (μM*h)	$t_{1/2}$ (h)	*F*%[d]
9	130	1.2	0.07	0.25	0.2	40%

See the Supplementary Data for experimental details associated with each assessment. Data reported are the arithmetic means from the dosing cohorts (Sprague-Dawley rats, n = 3/dose). Dosed at 1.5 mg/kg po (37/63 suspension of DMSO/MCT) and 0.5 mg/kg iv (25/60/15 solution of DMSO/PEG400/saline). [a]Observed plasma clearance (CL_p). [b]Volume of distribution (V_d). [c]Maximum plasma concentration (C_{max}). [d]Oral bioavailability (*F*%) was calculated according to the equation *F*% = (dose normalized AUC_{po})/(dose normalized AUC_{iv}). CL_p, V_d, and $t_{1/2}$ were derived from an iv study and C_{max}, AUC, and *F*% were derived from a po study.

In conclusion, we evolved a literature series of RORc inverse agonists (*i.e.* **1**) into a series of imidazo[1,5-*a*]pyridine and -pyrimidines with improved selectivity for RORc over PPARγ. Several compounds within the imidazo[1,5-*a*]pyridine and -pyrimidine series demonstrated potent RORc inverse agonist activity in biochemical and cellular assays. The most potent compounds also displayed >300-fold selectivity for RORc over the other ROR family members and NRs in our cellular selectivity panel. The favorable potency, selectivity, and physiochemical properties of GNE-0946 (**9**) and GNE-6468 (**28**), in addition to their potent suppression of IL-17 production in human primary cells, support their use as chemical biology tools to further explore the role of RORc in human biology.[48]

Supplementary data

Supplementary data associated with this article can be found, in the online version, at http://INSERT URL HERE

Acknowledgements

We thank Drs. Krista Bowman and Jiansheng Wu, and their respective Genentech research groups, for performing all required protein expression and purification activities.

References and Notes

1) Langley, R. G.; Elewski, B. E.; Lebwohl, M.; Reich, K.; Griffiths, C. E. M.; Papp, K.; Luig, L.; Nakagawa, H.; Spelman, L.; Sigrgeirsson, B.; Rivas, E.; Tsai, F.-F.; Wasel, N.; Tyring, S.; Salko, T.; Hamele, I.; Notter, M.; Karpov, A.; Helou, S.; Papavassilis, C. *N. Engl. J. Med.* **2014**, *371*, 326.
2) Papp, K. A.; Leonardi, C.; Menter, A.; Ortonne, J. P.; Krueger, J. G.; Kricorian, G.; Aras, G.; Li, J.; Russell, C. B.; Thompson, E. H.; Baumgartner, S. *N. Engl. J. Med.* **2012**, *366*, 1181.
3) Leonardi, C.; Matheson, R.; Zachariae, C.; Cameron, G.; Li, L.; Edson-Heredia, E.; Braun, D.; Banerjee, S. *N. Engl. J. Med.* **2012**, *366*, 1190.
4) Kellner, H. *Ther. Adv. Musculoskel. Dis.* **2013**, *5*, 141.
5) Baeten, D.; Baraliakos, X.; Braun, J.; Sieper, J.; Emery, P.; van der Heijde, D.; McInnes, I.; van Laar, J. M.; Landewé, R.; Wordsworth, P.; Wollenhaupt, J.; Kellner, H.; Paramarta, J.; Wei, J.; Brachat, A.; Bek, S.; Laurent, D.; Li, Y.; Wang, Y.; Bertolino, A. P.; Gseiger, S.; Wright, A. M.; Hueber, W. *Lancet* **2013**, *382*, 1705.
6) Hueber, W.; Patel, D. D.; Dryja, T.; Wright, A. M.; Koroleva, I.; Bruin, G.; Antoni, C.; Draelos, Z.; Gold, M. H.; Durez, P.; Tak, P. P.; Gomez-Reino, J. J.; Foster, C. S.; Kim, R. Y.; Samson, C. M.; Falk, N. S.; Chu, D. S.; Callanan, D.; Nguyen, Q. D.; Rose, K.; Haider, A.; Di Padova, F. *Sci. Transl. Med.* **2010**, *2*, 52ra72.
7) Griffiths, C. E. M.; Strober, B. E.; van de Kerkhof, P.; Ho, V.; Fidelus-Gort, R.; Yeilding, N.; Guzzo, C.; Xia, Y.; Zhou, B.; Li, S.; Dooley, L. T.; Goldstein, N. H.; Menter, A. *N. Engl. J. Med.* **2010**, *362*, 118.

8) FDA approves new psoriasis drug Cosentyx. http://www.fda.gov/NewsEvents/Newsroom/PressAnnouncements/ucm430969.htm (accessed Feb 9, 2015).

9) Bartlett, H. S.; Million, R. P. *Nat. Rev. Drug Discov.* **2015**, *14*, 11.

10) Pappu, R.; Ramirez-Carrozzi, V.; Ota, N.; Ouyang, W.; Hu, Y. *J. Clin. Immunol.* **2010**, *30*, 185.

11) Hirose, T.; Smith, R. J.; Jetten, A. M. *Biochem. Biophys. Res. Commun.* **1994**, *205*, 1976.

12) Ivanov, I. I.; McKenzie, B. S.; Zhou, L.; Tadokoro, C. E.; Lepelley, A.; Lafaille, J. J.; Cua, D. J.; Littman, D. R. *Cell* **2006**, *126*, 1121.

13) Sabat, R.; Ouyang, W.; Wolk K. *Nat. Rev. Drug Discov.* **2014**, *13*, 21.

14) Cording, S.; Medvedovic, J.; Cherrier, M.; Eberl, G. *FEBS Letters* **2014**, *588*, 4176.

15) Eberl, G.; Marmon, S.; Sunshine, M.-J.; Rennert, P. D.; Choi, Y.; Littman, D. R. *Nat. Immunol.* **2004**, *5*, 64.

16) Pantelyushin, S.; Haak, S.; Ingold, B.; Kulig, P.; Heppner, F. L.; Navarini, A. A.; Becher, B. *J. Clin. Invest.* **2012**, *122*, 2252.

17) Williams, S. C. P. *Nat. Med.* **2013**, *19*, 1078.

18) Yang, J.; Sundrud, M. S.; Skepner, J.; Yamagata, T. *Trends Pharmacol. Sci.* **2014**, *35*, 493.

19) Isono, F.; Fujita-Sato, S.; Ito, S. *Drug Disc. Today* **2014**, *19*, 1205.

20) Fauber, B. P.; Magnuson, S. *J. Med. Chem.* **2014**, *57*, 5871.

21) Kojetin, D. J.; Burris, T. P. *Nat. Rev. Drug Discov.* **2014**, *13*, 197.

22) Kamenecka, T. M.; Lyda, B.; Chang, M. R.; Griffin, P. R. *Med. Chem. Commun.* **2013**, *4*, 764.

23) Dhar, T. G. M.; Zhao, Q.; Markby, D. W. *Annu. Rep. Med. Chem.* **2013**, *48*, 169.

24) René, O.; Fauber, B. P.; Boenig, G.; Burton, B.; Eidenschenk, C.; Everett, C.; Gobbi, A.; Hymowitz, S. G.; Johnson, A. R.; Kiefer, J. R.; Liimatta, M.; Lockey, P.; Norman, M.; Ouyang, W.; Wallweber, H. A.; Wong, H. *ACS Med. Chem. Lett.* **2015**, *6*, 276.

25) van Niel, M. B.; Fauber, B. P.; Cartwright, M.; Gaines, S.; Killen, J. C.; René, O.; Ward, S. I.; Boenig, G.; Deng, Y.; Eidenschenk, C.; Everett, C.; Gancia, E.; Ganguli, A.; Gobbi, A.; Hawkins, J.; Johnson, A. R.; Kiefer, J. R.; La, H.; Lockey, P.; Norman, M.; Ouyang, W.; Qin, A.; Wakes, N.; Waszkowycz, B.; Wong, H. *Bioorg. Med. Chem. Lett.* **2014**, *24*, 5769.

26) Fauber, B. P.; René, O.; Boenig, G.; Burton, B.; Deng, Y.; Eidenschenk, C.; Everett, C.; Gobbi, A.; Hymowitz, S. G.; Johnson, A. R.; La, H.; Liimatta, M.; Lockey, P.; Norman, M.; Ouyang, W.; Wang, W.; Wong, H. *Bioorg. Med. Chem. Lett.* **2014**, *24*, 3891.

27) Fauber, B. P.; René, O.; Burton, B.; Everett, C.; Gobbi, A.; Hawkins, J.; Johnson, A. R.; Liimatta, M.; Lockey, P.; Norman, M.; Wong, H. *Bioorg. Med. Chem. Lett.* **2014**, *24*, 2182.

28) Karstens, W. F. J.; van der Stelt, M.; Cals, J.; Azevedo, R. C. R. G.; Barr, K. J.; Zhang, H.; Beresis, R. T.; Zhang, D.; Duan, X. WO 2012/106995, Aug 16, 2012.

29) *See* the Supplementary Data section of the following reference for the detailed biochemical and cellular assay protocols: Fauber, B. P.; Boenig, G.; Burton, B.; Eidenschenk, C.; Everett, C.; Gobbi, A.; Hymowitz, S. G.; Johnson, A. R.; Liimatta, M.; Lockey, P.; Norman, M.; Ouyang, W.; René, O.; Wong, H. *Bioorg. Med. Chem. Lett.* **2013**, *23*, 6604.

30) (a) Acton, J. J.; Akiyama, T. E.; Chang, C. H.; Colwell, L.; Debenham, S.; Doebber, T.; Einstein, M.; Liu, K.; McCann, M. E.; Moller, D. E.; Muise, E. S.; Tan, Y.; Thompson, J. R.; Wong, K. K.; Wu, M.; Xu, L.; Meinke, P. T.; Berger, J. P.; Wood, H. B. *J. Med. Chem.* **2009**, *52*, 3846. (b) Acton, J. J.; Black, R. M; Jones, A. B.; Moller, D. E.; Colwell, L.; Doebber, T. W.; MacNaul, K. L.; Berger, J.; Wood, H. B. *Bioorg. Med. Chem. Lett.* **2005**, *15*, 357.

31) The human PPARγ-LBD fluorescence polarization binding assay was conducted using the Life Technologies (ThermoFisher Scientific Corp., Grand Island, NY) "Polar-Screen^{TM} PPAR Gamma Competitor Assay, Green" assay kit (catalog number PV6136). For additional details on this assay, *see*: https://tools.lifetechnologies.com/content/sfs/manuals/Polar_Screen_PPARgamma_competitor_Assay_Green_PI.pdf (accessed Feb 12, 2015).

32) Sohda, T.; Momose, Y.; Meguro, K.; Kawamatsu, Y.; Sugiyama, Y.; Ikeda, H. *Arzneim.-Forsch.* **1990**, *40*, 37.

33) Fujiwara, T.; Yoshioka, S.; Yoshioka, T.; Ushiyama, I.; Horikoshi, H. *Diabetes* **1988**, *37*, 1549.

34) Graham, D. J.; Ouellet-Hellstrom, R.; MaCurdy, T. E.; Ali, F.; Sholley, C.; Worrall, C.; Kelman, J. A. *JAMA* **2010**, *304*, 411.

35) Liu, K.; Black, R. M.; Acton, J. J.; Mosley, R.; Debenham, S.; Abola, R.; Yang, M.; Tschirret-Guth, R.; Colwell, L.; Liu, C.; Wu, M.; Wang, C. F.; MacNaul, K. L.; McCann, M. E.; Moller, D. E.; Berger, J. P.; Meinke, P. T.; Jones, B.; Wood, H. B. *Bioorg. Med. Chem. Lett.* **2005**, *15*, 2437.

36) For representative synthetic protocols and characterization of the analogs, *see* Fauber, B. P.; Gobbi, A. WO 2015/036411, Mar 19, 2015. The synthesis and characterization of **9** (GNE-0946) and **28** (GNE-6468) are described in the Supplementary Data section of this manuscript.

37) Leeson, P. D.; Springthorpe, B. *Nat. Rev. Drug Discov.* **2007**, *6*, 881.

38) Leach, A. R.; Hann, M. M.; Burrows, J. N.; Griffen, E. J. *Mol. BioSyst.* **2006**, *2*, 429.

39) The partition coefficient (LogP) was calculated with internal software using the VolSurf approach. For additional details, s*ee* Cruciani, G.; Crivori, P.; Carrupt, P.-A.; Testa, B. *THEOCHEM* **2000**, *503*, 17.

40) A similar improvement in potency was noted in a recent 1-acyl-indazole patent application from Merck. For additional details, see Barr, K. J.; MacLean, J.; Zhang, H.; Beresis, R. T. WO 2014/028600, Feb 20, 2014.

41) Sundrud, M. S.; Rao, A. *Immunity*, **2008**, *28*, 5.

42) Yang, X. O.; Pappu, B. P.; Nurieva, R.; Akimzhanov, A.; Kang, H. S.; Chung, Y.; Ma, L.; Shah, B.; Panopoulos, A. D.; Schluns, K. S.; Watowich, S. S.; Tian, Q.; Jetten, A. M.; Dong, C. *Immunity* **2008**, *28*, 29.

43) *In vitro* assays to explore the themes of cellular permeability and predicted metabolic clearance have been referred to as *in vitro* ADME assays. For additional discussion, *see* Tarbit, M. H.; Berman, J. *Curr. Opin. Chem. Biol.* **1998**, *2*, 411.

44) *See* the Supplementary Data section of Ref. 26 for the *in vitro* ADME assay protocols.

45) Irvine, J. D.; Takahashi, L.; Lockhart, K.; Cheong, J.; Tolan, J. W.; Selick, H. E.; Grove, J. R. *J. Pharm. Sci.* **1999**, *88*, 28.

46) Krishna, D. R.; Klotz, U. *Clin. Pharmacokinet.* **1994**, *26*, 144.

47) (a) Das, S.; Thomas, A.; Khairatkar-Joshi, N.; Shah, D. M.; Bajpai, M. WO 2015/052675, Apr 16, 2015. (b) Chaudhari, S. S.; Thomas, A.; Shone, S. V.; Khairatkar-Joshi, N.; Bajpai, M. WO 2015/008234, Jan 22, 2015.

48) GNE-0946 (**9**) and GNE-6468 (**28**) can be requested through the Genentech Research Contracts and Reagents Program (https://www.gene.com/gene/reagents-program/request.do).

Graphical Abstract.

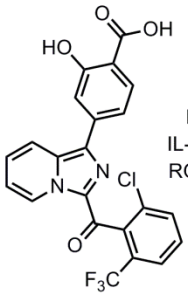

GNE-0946
(**9**)
RORc Cell EC_{50} = 4 nM
IL-17 hPBMC EC_{50} = 17 nM
RORc Selectivity = 325-fold

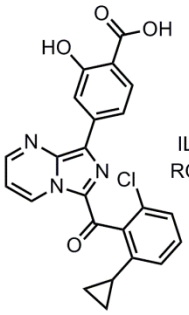

GNE-6468
(**28**)
RORc Cell EC_{50} = 13 nM
IL-17 hPBMC EC_{50} = 30 nM
RORc Selectivity > 1,000-fold